Preparatory Consultancy Meeting for the Injected Impurities, IAEA CRP

Naoko ASHIKAWA (NIFS, SOKENDAI)

Thanks for T.Oishi(NIFS), Z.S.Yang (ASIPP)

June 7, 2022, Remote meeting

Requests from IAEA-1

What data are needed for modelling the atomic and molecular physics of injected impurities?

Are impurities both for power mitigation and for **plasma diagnostics** in scope?

Which species should be in scope: certainly, N and Ne (maybe also Ar?)
for power control in the divertor area; Li, B and BN for edge plasma regions; others?
>>these materials are used for turbulence control (B) and impurity and hydrogen recycling control (B, Li)
*Method 1; pellet, 2; IPD, 3; gas,
4;Laser ablation (no page, for example SWIP in China)
Which processes are of greatest importance (collisions with H/D/T/He/e-, radiative line strengths), and which energy ranges (1 – 100 eV up to several keV for ELMs)?

What is the importance of molecules to the CRP, e.g. in the formation of NHx isotopologues in the sub-divertor region?

How are data incorporated into models like SOLPS-ITER and how can integration of new data be facilitated?

Method1; Spectroscopy and tungsten pellet injection in LHD

LHD

- Bt < 3 T, R = 3.6 m, <a> = 0.64 m
- Toroidal/poloidal period number = 10/2
- Heating: ECRH, NBI
  - negative ion source (**n-NBI**): NBI#1, #2, #3
  - positive ion source (**p-NBI**): NBI#4, #5

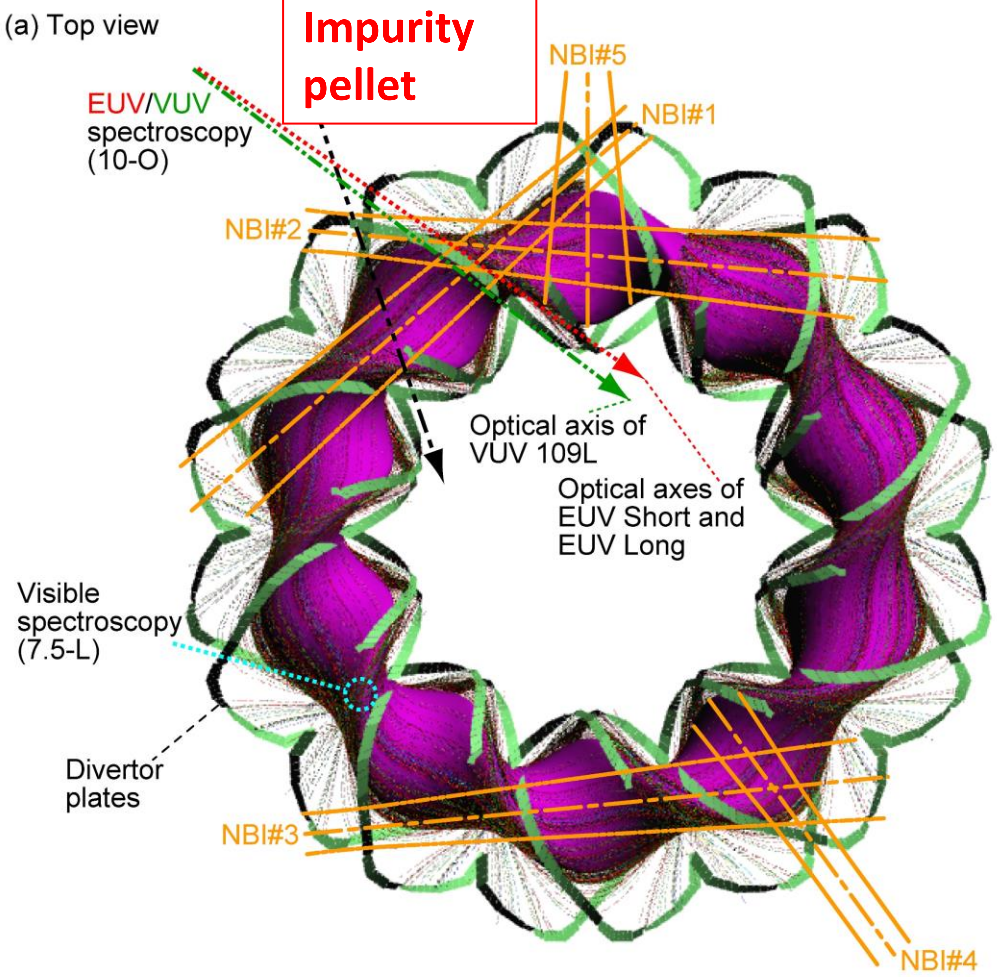

Impurity pellet

- W wire in a C pellet: l0.7 mm x ϕ0.1 mm ~3.5 × 10^{17} W atoms

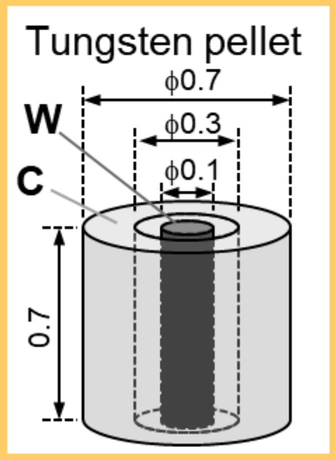

Spectroscopy

- Visible MK300: 3200–3550 Å
- VUV 109L: 250–1050 Å
- EUV Long: 100–300 Å
- EUV Short: 5–60 Å

LHD has two types of impurity pellet, “impurity pellet” and, “TESPEL” (Tracer-Encapsulated Solid Pellet)

T.Oishi

Introduction: Tungsten behavior in fusion plasmas

T.Oishi

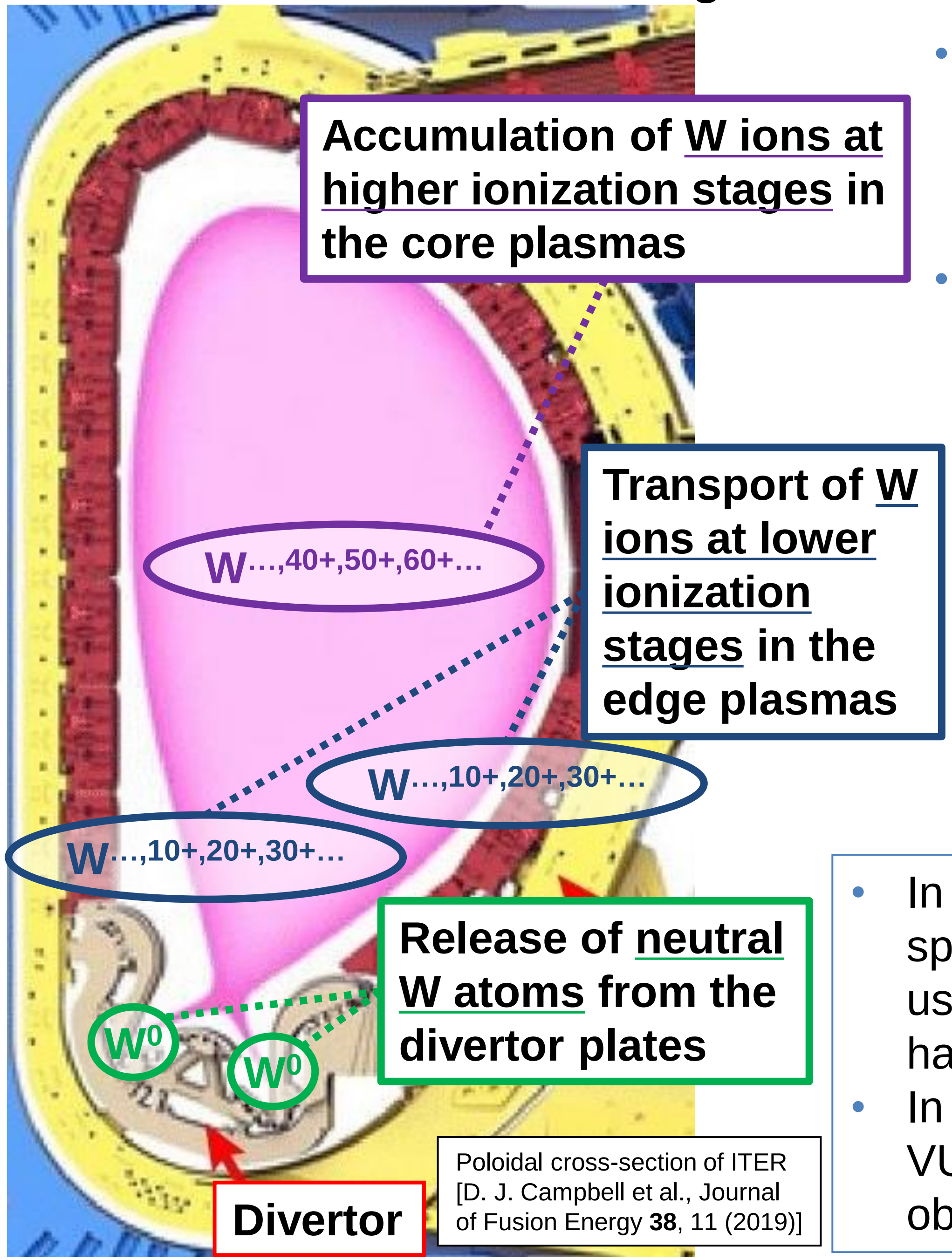

Poloidal cross-section of ITER [D. J. Campbell et al., Journal of Fusion Energy **38**, 11 (2019)]

- Tungsten is regarded as a leading candidate material for the plasma facing component in ITER and future fusion reactors.
- Spectroscopic studies for tungsten impurity ions in magnetically-confined high-temperature plasmas…

Neutral W atoms: Visible spectroscopy
W ions at lower ionization stages: VUV spectroscopy
W ions at higher ionization stages: EUV spectroscopy, SX imaging

- In the Large Helical Device (LHD), spectroscopic studies for tungsten ions using a tungsten pellet injection technique have been intensively conducted.
- In this talk, the tungsten spectra in visible, VUV, and EUV wavelength ranges observed in LHD will be summarized.

T.Oishi

Application of the observation

(i) Temporal evolution of the W^0–W^{46+} emission

- **W^0, W^{5+}, W^{6+}, W^{24+}–W^{28+}, W^{37+}, W^{38+}, and W^{41+}–W^{46+}** line emissions were picked up as useful emission lines to monitor temporal evolution of emission intensity in a wide range of the charge states.
- The dominant charge state varied sequentially in time, together with T_{e0}. It is a reasonable relationship between T_e and the ionization energy, E_i.
- **W^{10+}–W^{20+}** emission data are insufficient.

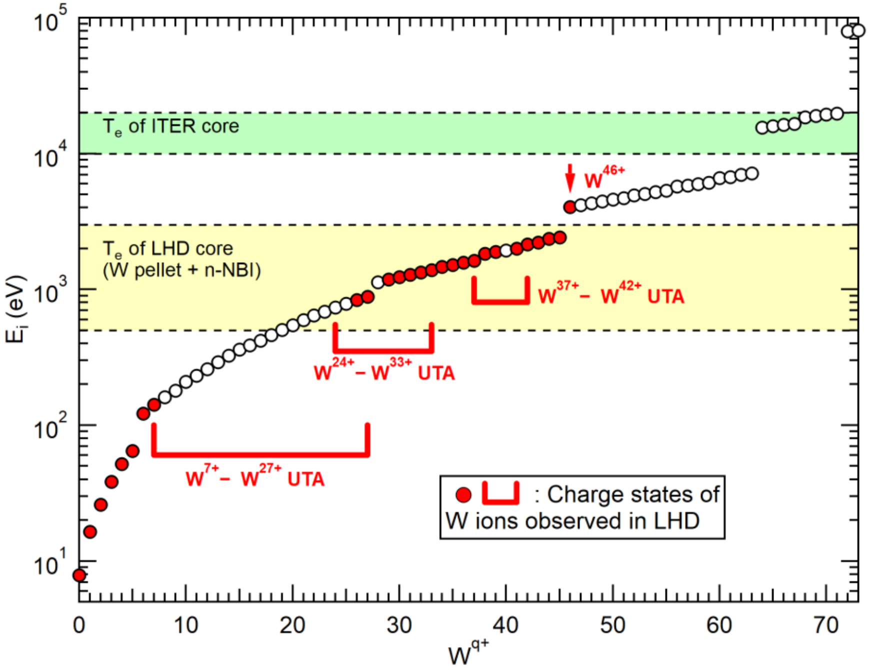

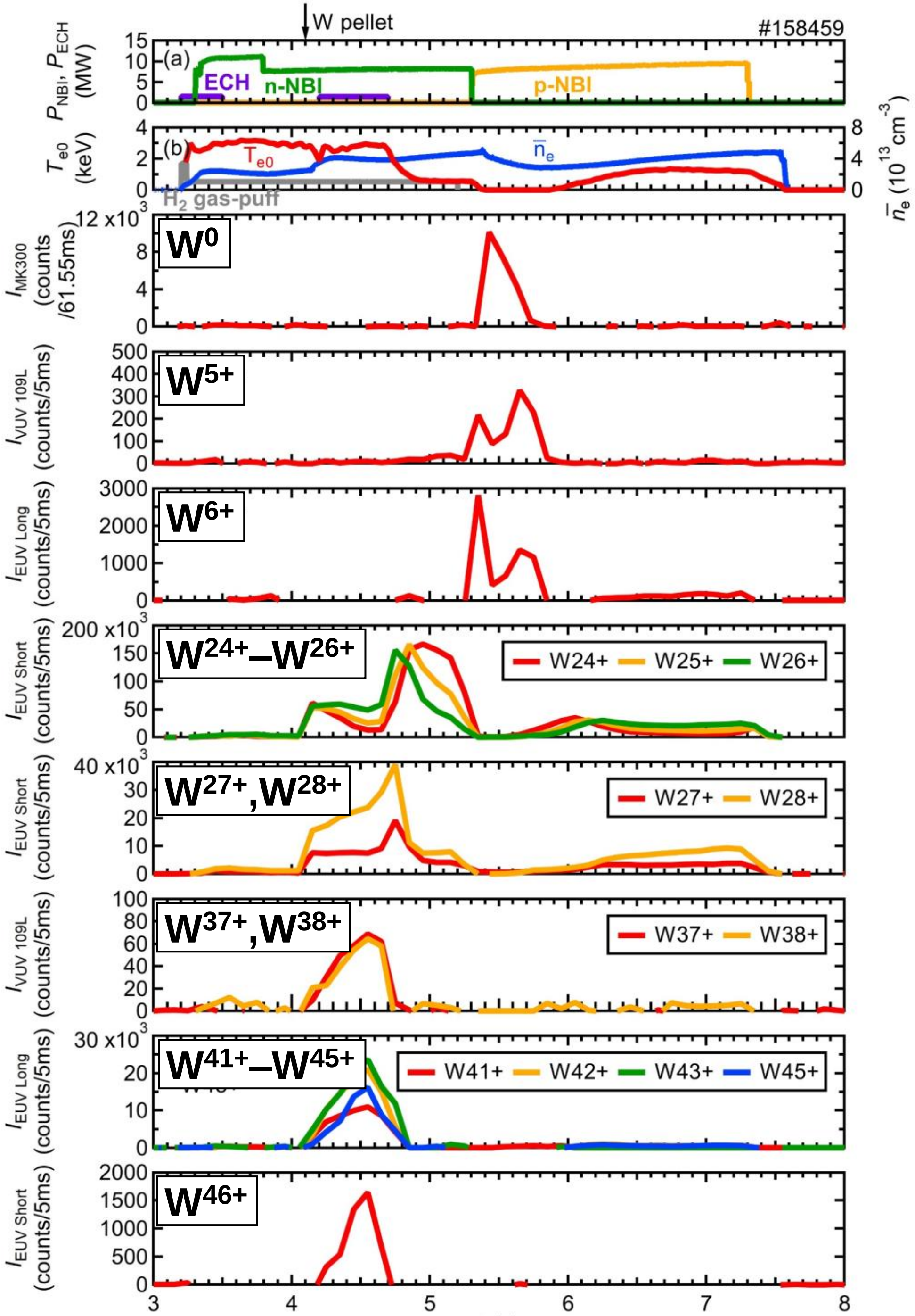

[T. Oishi et al., Atoms **9**, 69 (2021)]

Method 2; Impurity powder dropper (IPD）

IPD was developed in PPPL and IPD-LHD experiments were started in 2019.

Powders are served to plasmas by the gravity force. A distance from the cup of powders to plasmas is more than 3 m

Dropped amounts of powders were controlled by the piezo vibration. At present, two materials, B and BN can be dropped in LHD

- $2\sim 50$ g **boron (B)** $\emptyset = \sim 100\ \mu$m

Boron powder

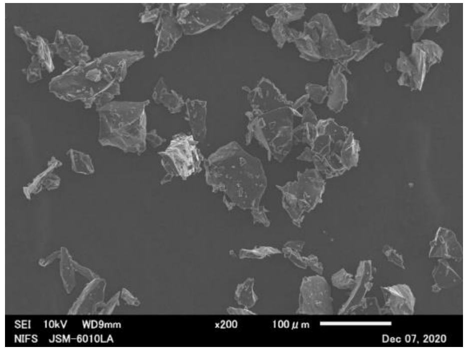

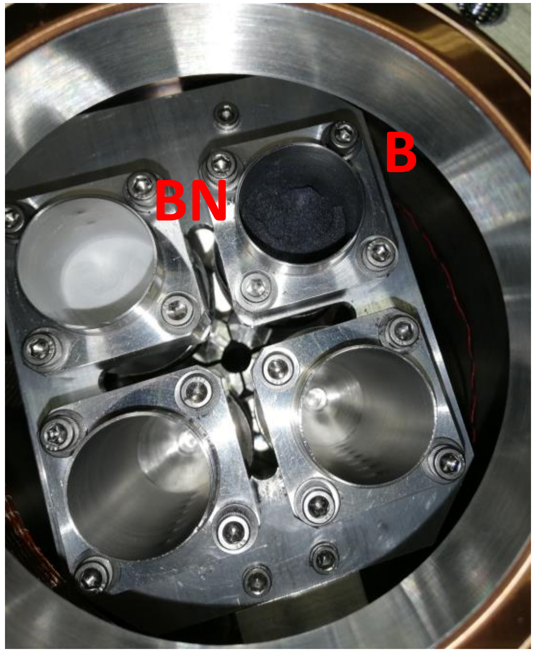

IPD system in LHD

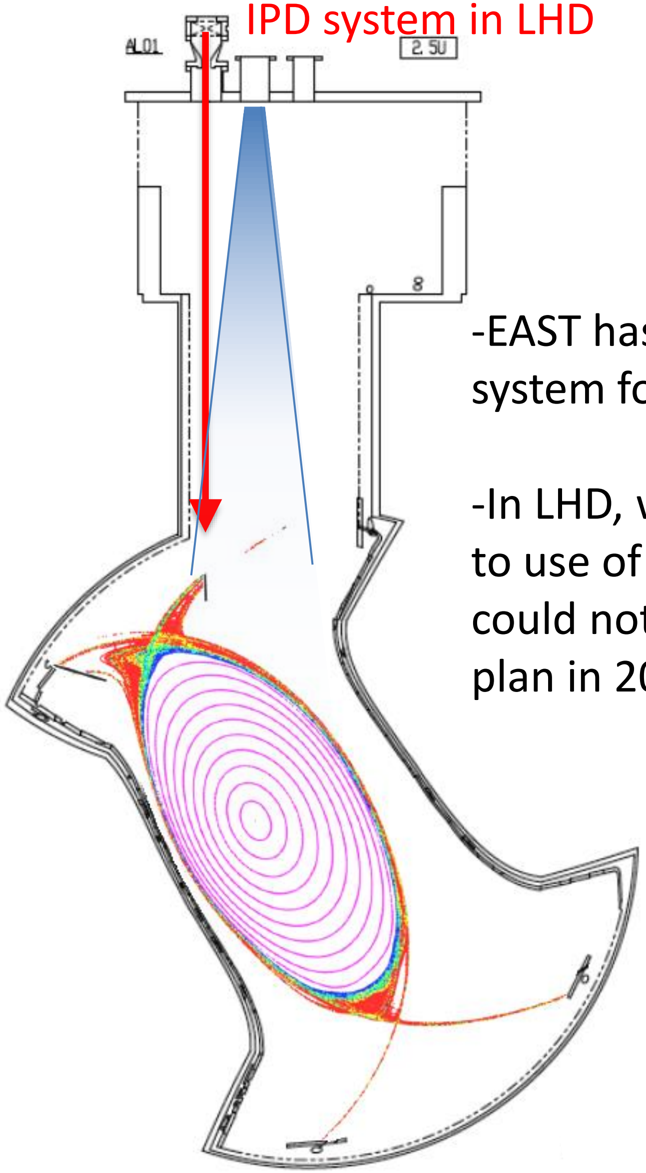

-EAST has the similar system for Li

-In LHD, we planed to use of Li, but could not use it. It plan in 2022.

IPD : Visible camera observation

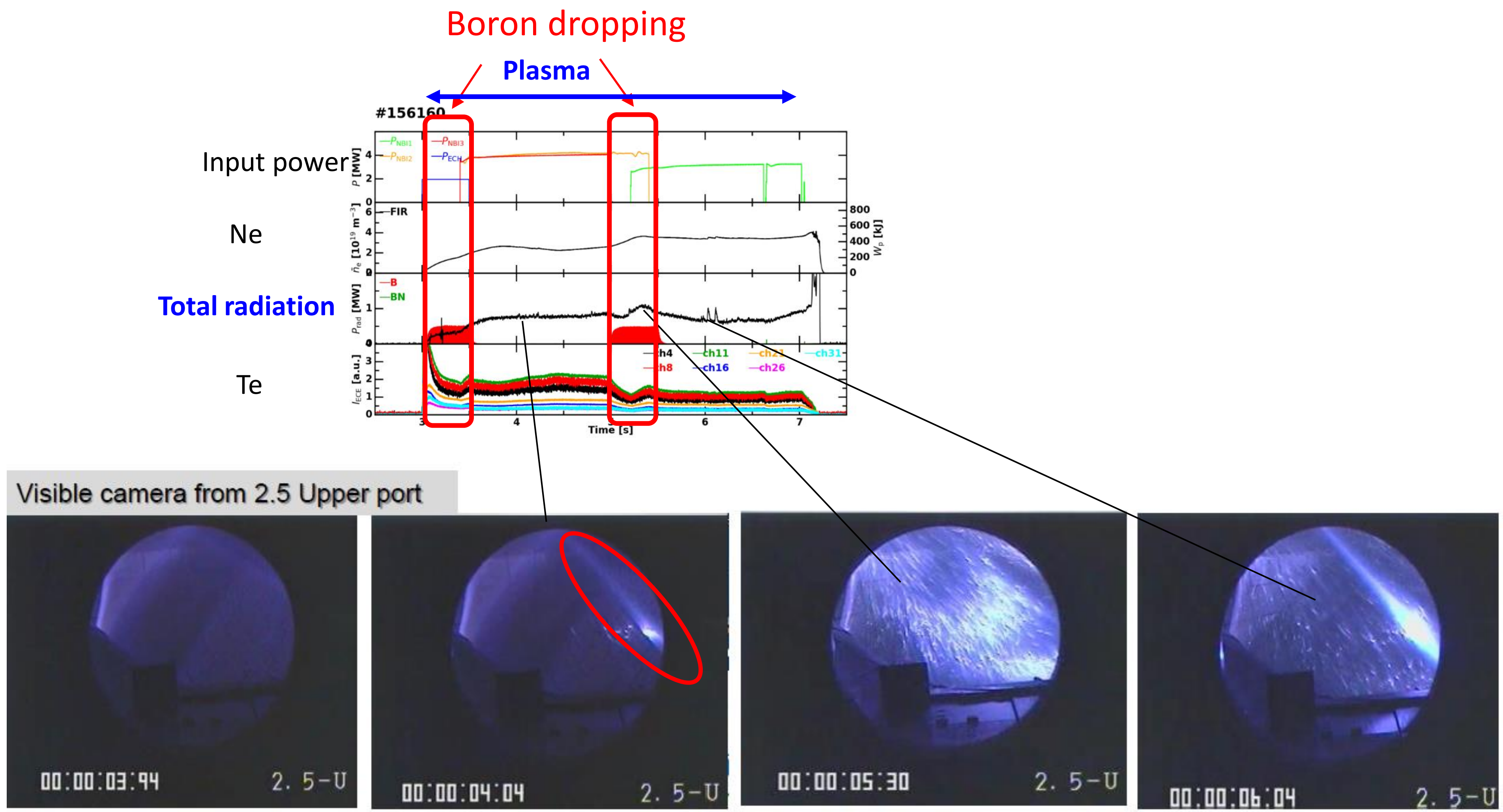

3:44s | 4:04s | 5:30s | 6:04s

Starting time of Piezo vibration from 3s.
Starting time of brightness due to dropped powders about 4s.

Spatial profiles of boron intensities (IPD)

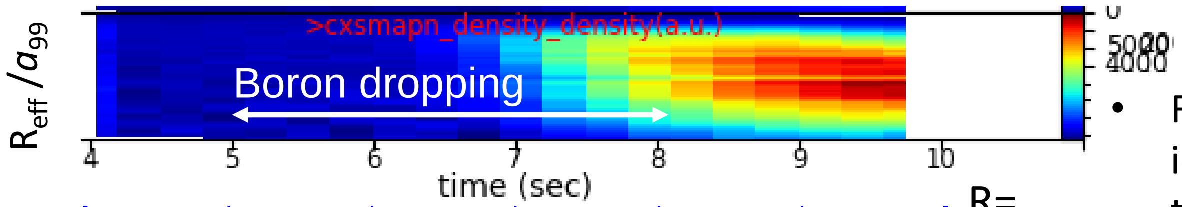

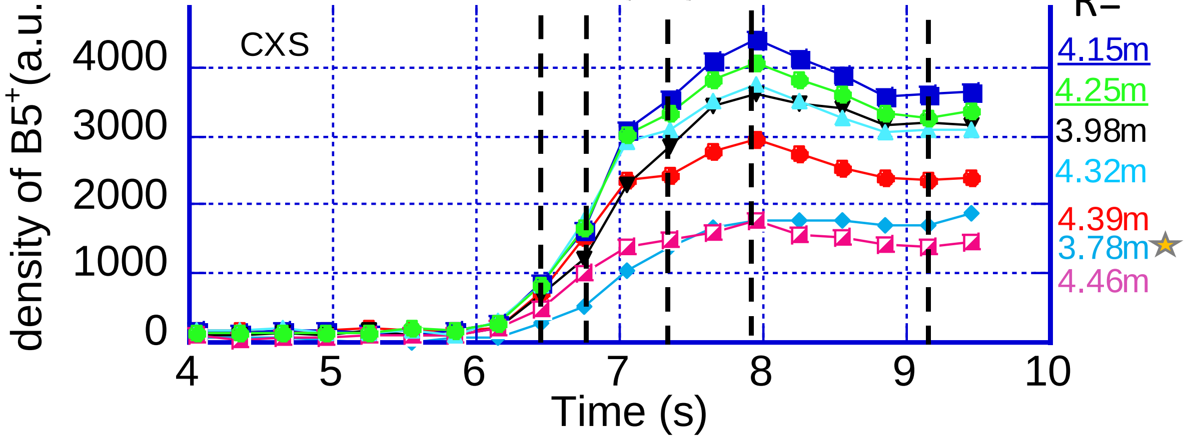

- From CXS observations, ionized boron is observed in the core plasmas.
- In R_{eff}/a_{99}= 0.6-0.8, density was increasing during B powder dropping
- In core region less than R_{eff}/a_{99}= 0.4, time evaluation is slower to compare with that in the outer region. The density level was kept after stopped the B dropping.

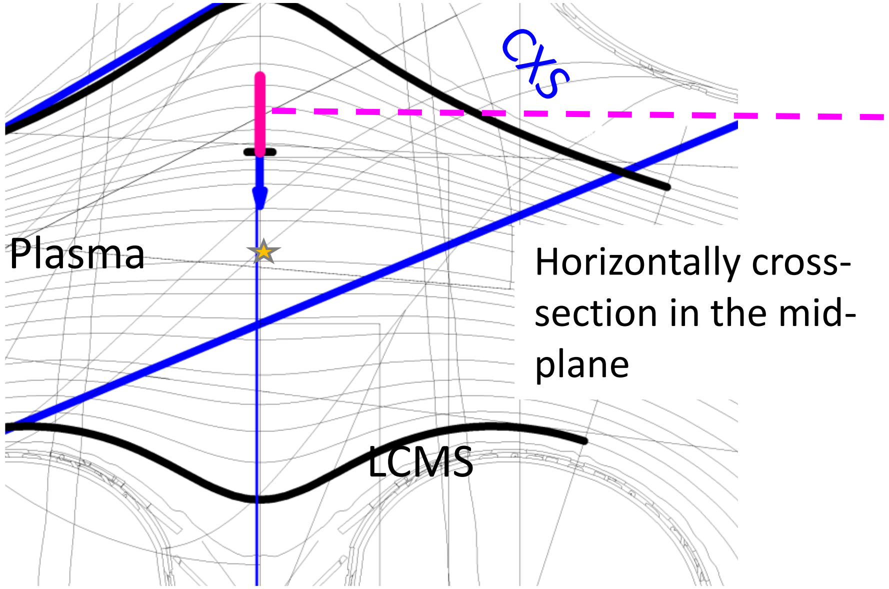

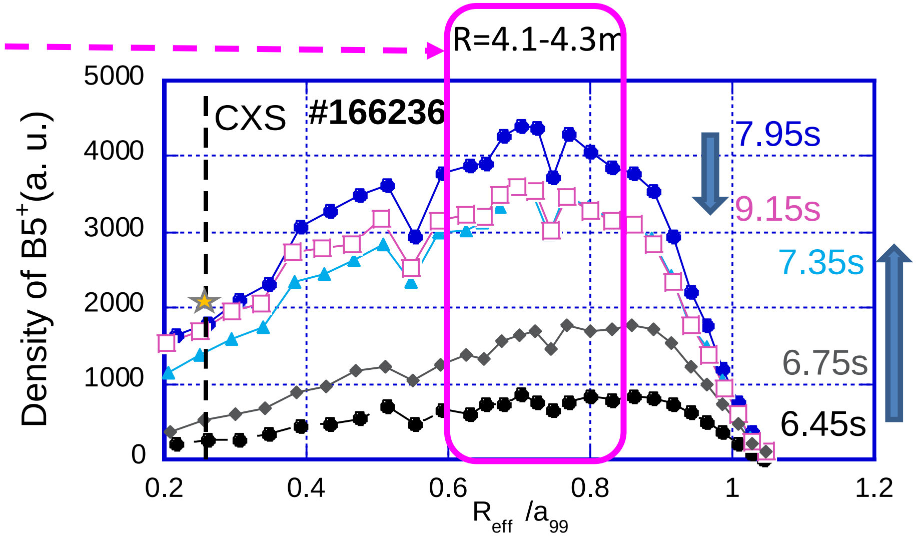

Boron dropping in EAST

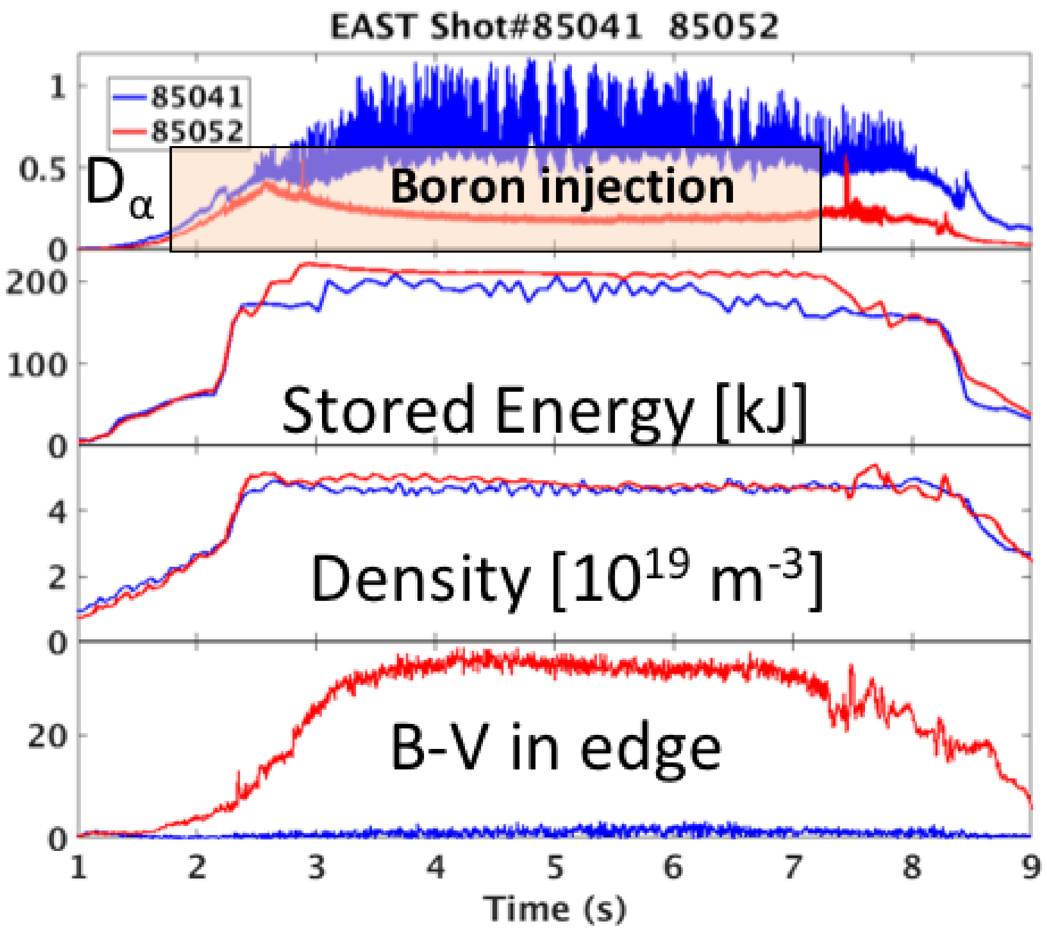

- No Boron (#85041)
- Boron injection above a threshold
- Stored energy increased slightly
- Density matched
- B-V in edge shows when B injected

B, Li dropping in EAST (2021)

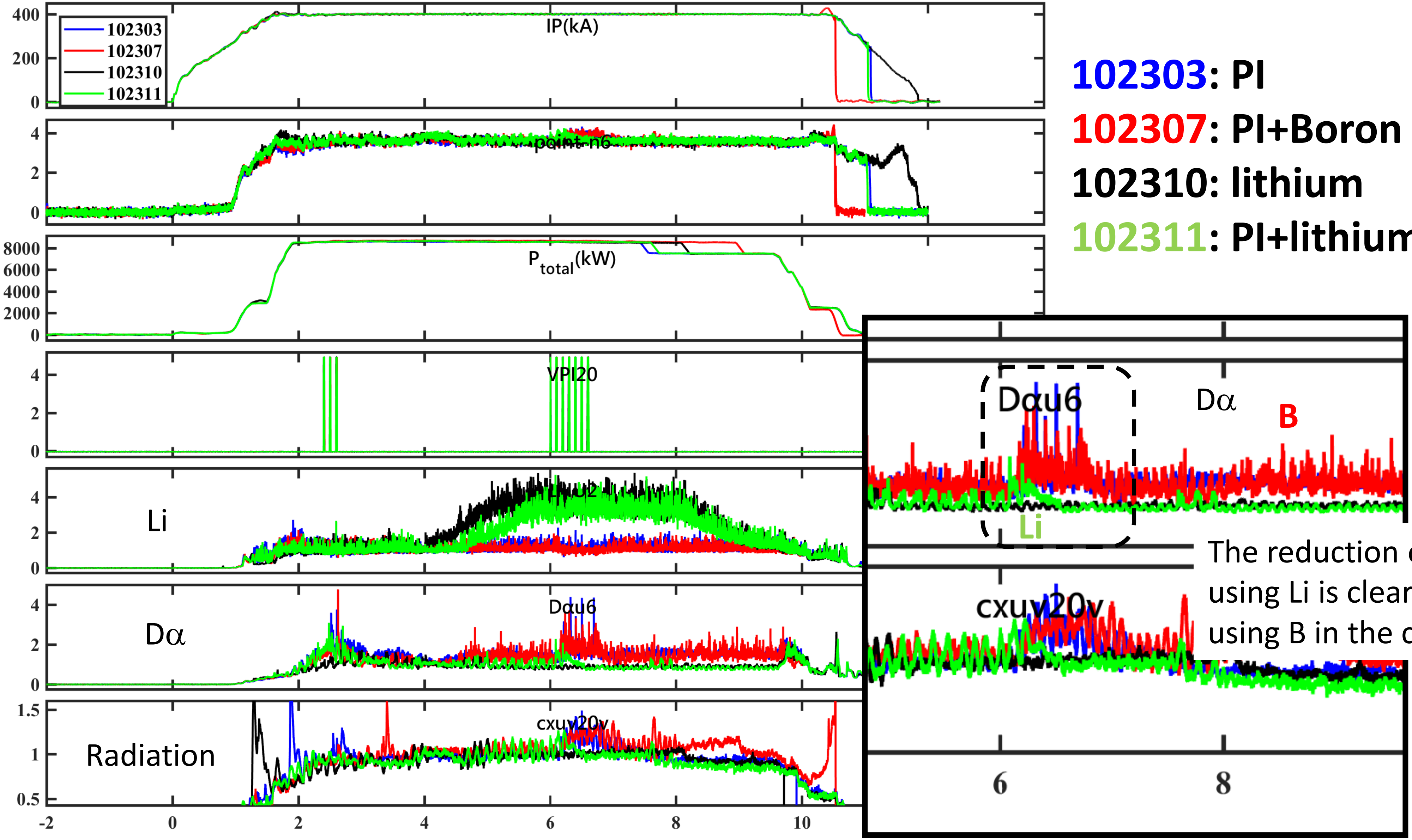

102303: PI

102307: PI+Boron

102310: lithium

102311: PI+lithium

The reduction of Dα using Li is clear that using B in the case.

N. Ashikawa (NIFS), Y.W.Yu(ASIPP)

B dropping in LHD

LHD 171050 (Bt, Rax, gamma, Bq) = (2.75, 3.6,

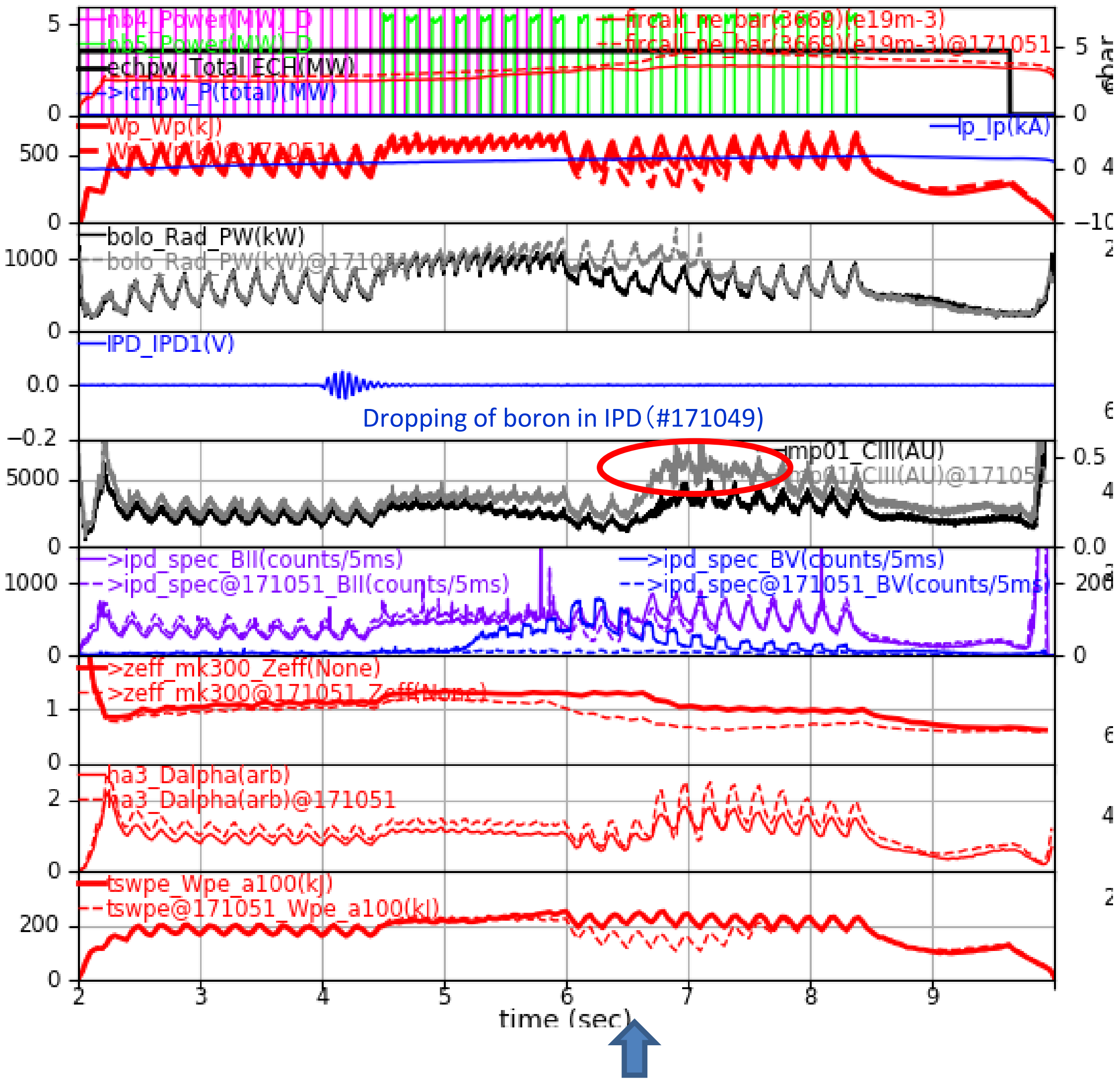

Increasing of CIII in the case of w/o boron at 7s。

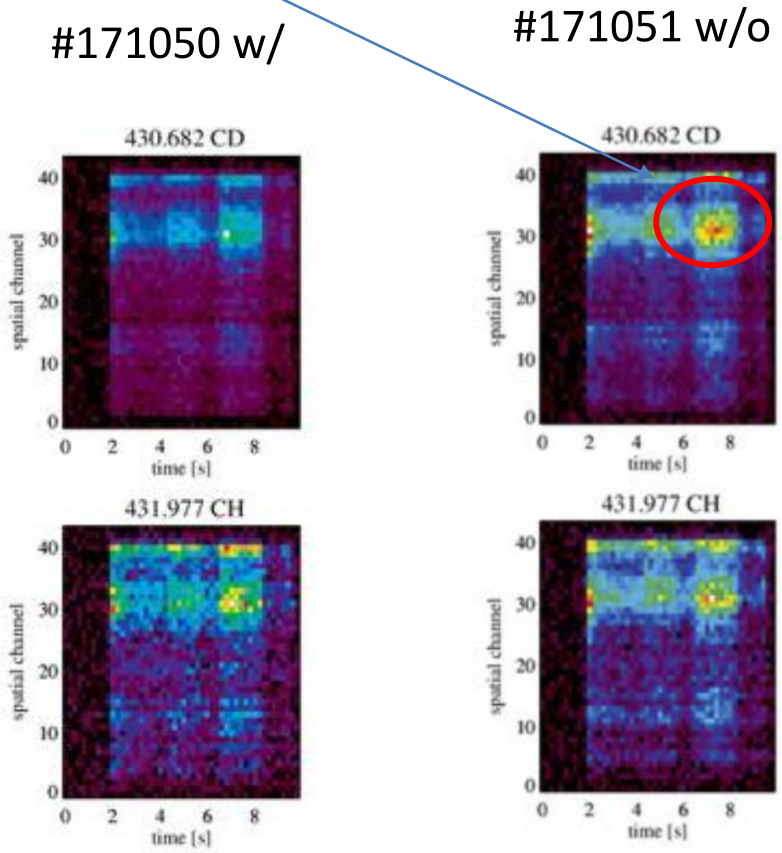

Increasing of CIII in the case of w/o boron
Kawate try to measure BH and CH lines

Supersonic Gas puff (SSGP) for both #171050 and #171051 at 6.5s. After SSGP, Da increases at w/o B. How about He discharge? <<In the request sheet, He SSGP is written.
If coating effect on the target is reason for a reduction of Da, it is might be useful for He.

Progress on analytical method; Ti of B using BII data

T. Oishi, et al.,

Plasma Sci. Technol. **23** (2021) 084002

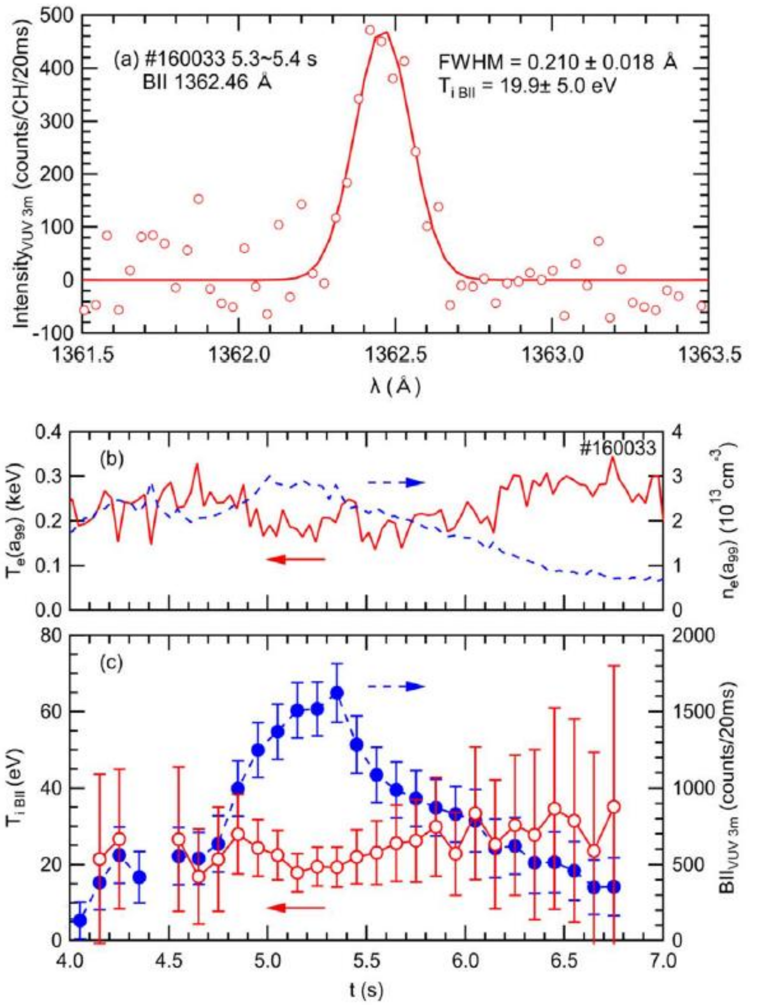

Figure 9. Ion temperature measurement of B^+ ions using a 3 m normal incidence VUV spectrometer. (a) Wavelength spectrum of BII 1362.46 Å together with a Gaussian function as a fitting curve. Temporal evolutions of (b) edge electron temperature $T_e(a_{99})$ and edge electron density $n_e(a_{99})$, and (c) the temperature of B^+ ions, $T_{i\ BII}$, and the emission intensity of the BII line. (d) Edge electron

The ion temperature Ti (eV) is provided by

Ti=1.68×10^8M (ΔFWHM/λ0)^2,

- M is the atomic mass number,
- ΔFWHM is the Doppler width at FWHM,
- λ0 is the central wavelength.

Comparison of different impurity injection:

Z.S.Yang

Ar/Ne puffing on the outer divertor target both achieve steady-state partial energy detachment

- I_p=400kA, P_{inj}=2MW, B_t=2.5T (Fav.)
- n_{el}~$4\times10^{19}m^{-3}$
- $H_{98,y2}$~1
- 50%Ar&50%D_2, 50%Ne&50%D_2
- $T_{et,UOSP}$~5eV, Peak $T_{div,UO}$ ↓

For energy detachment:

- ☐ Total number of impurity particles required: $N_{Ar}<N_{Ne}$
- ☐ Main plasma radiation increments: $\Delta P_{rad\text{-}bulk}(Ar)>\Delta P_{rad\text{-}bulk}(Ne)$

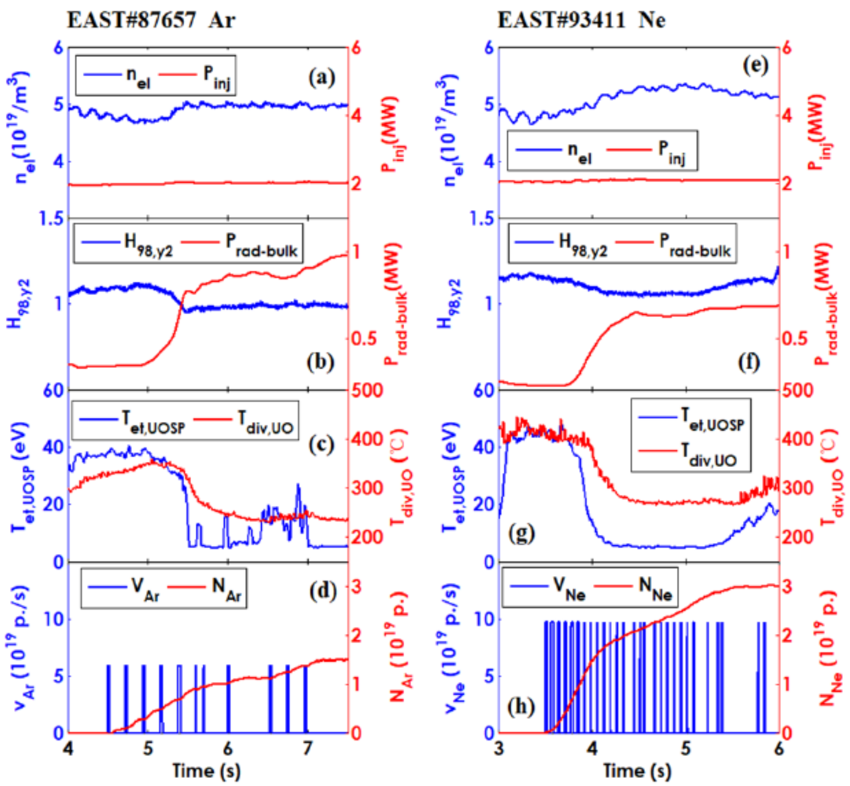

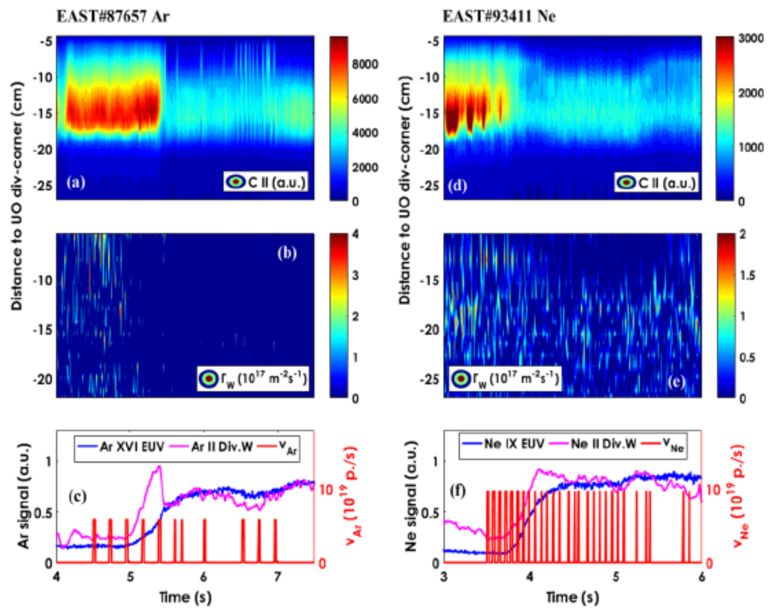

- Ar, Ne radiation ↑ by spec. data
- C radiation ↓
- Γ_W: ~$10^{17}m^{-2}s^{-1}$

➢ **Under current EAST operating conditions, better cooling capacity of Ar to the upper outer divertor and better compatibility between Ne and core plasma**

➢ **Both Ar and Ne injection effectively suppress the sputtering of the divertor target plate**

Z.S.Yang

Radiative divertor simulations for Ne seeding scenarios by using SOLPS code

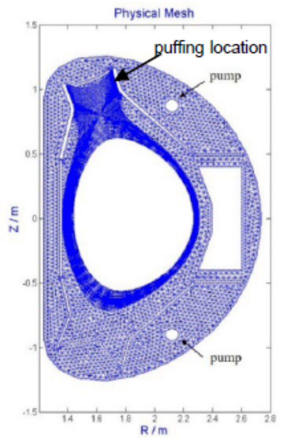

Computational mesh for Ne seeding for EAST #71021 (t=2.95s)

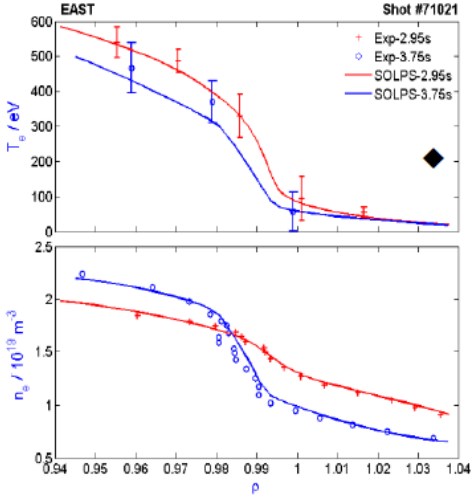

The upstream density and temperature

◆ The agreement between simulated midplane profiles and experimental results

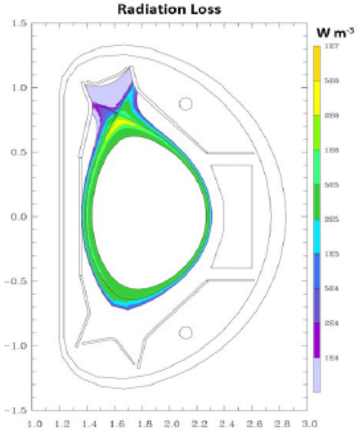

The modeled radiation distribution after Ne seeding (EAST #71021)

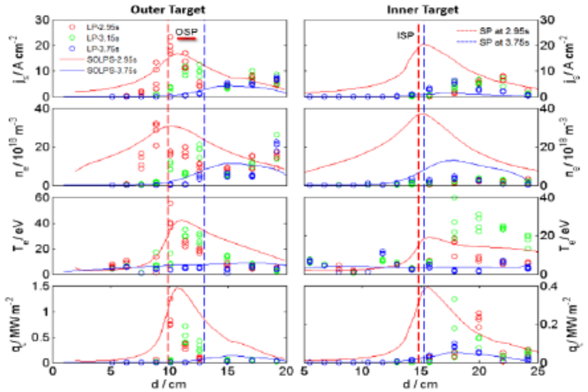

The density and temperature for outer /inner upper divertor target (experiments data vs. Simulation results)

Radiation distribution at different seeding rate

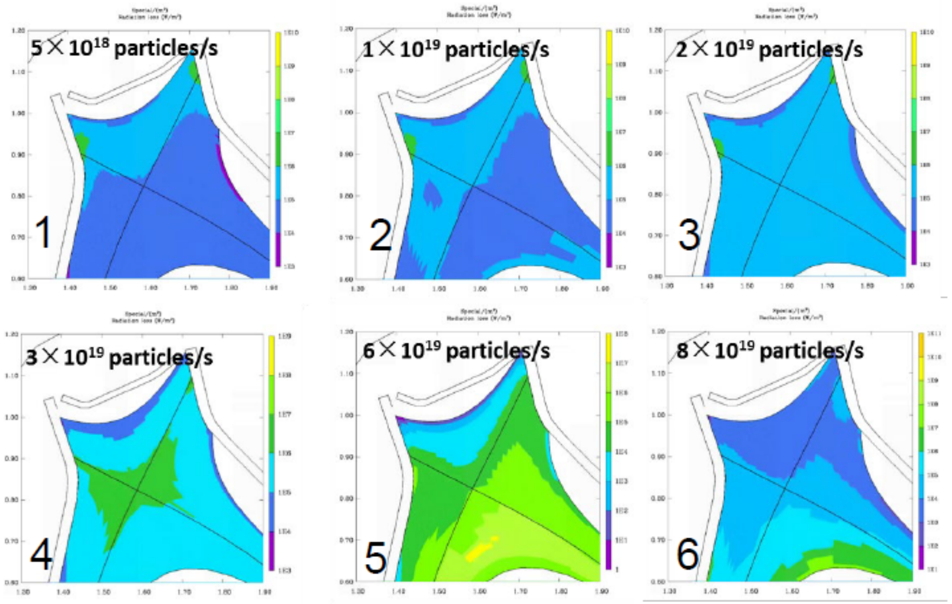

- ◆ **Lower** frad* (<40%): radiation mainly distributed in the divertor region (Fig.1-3) *frad=Prad/Ptotal
- ◆ **Medium** frad* (40%-65%): radiation mainly concentrated near the X point, and the MARFE phenomenon (Fig.4)
- ◆ **Higher** frad* (>65%) : Most of the radiation loss in the core region (Fig.5-6)

Z.S.Yang

Impurity injection system and relevant diagnostics on EAST

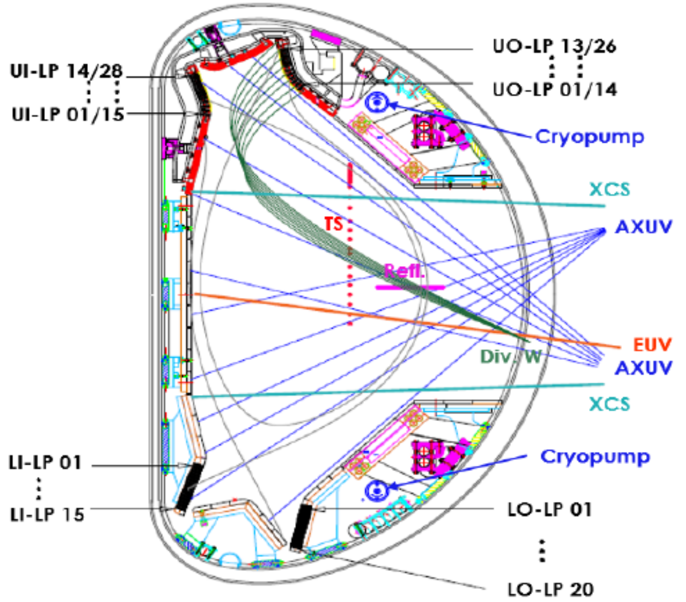

Diagnostics distribution for impurity injection experiments

- Divertor probe: j_s, T_e, n_e, q_t, p_{total} on the divertor target
- InfraRed camera: T_{div}, q_t on the divertor target
- Divertor tungsten spectrum: C, Ne, Ar, W in diverter region
- Extreme UltraViolet spectrometer, EUV: C, Ne, Ar, W in midplane
- Absolute eXtreme UltraViolet bolometer arrays, AXUV: radiation distribution
- Microwave reflectometer: n_e in midplane
- Thomson Scattering, TS: Te in the core and boundary
- X-ray crystal spectroscopy, XCS: Ti in the core
- POINT: ne in the core

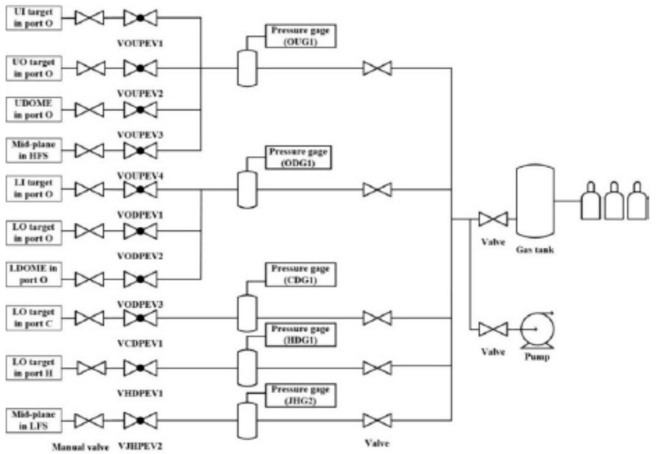

Impurity gas puffing system on EAST

- Impurity gas puffing system consists of: pipe, shut-off valve, piezoelectric valve, pressure stabilization tank, pressure gage and pump.

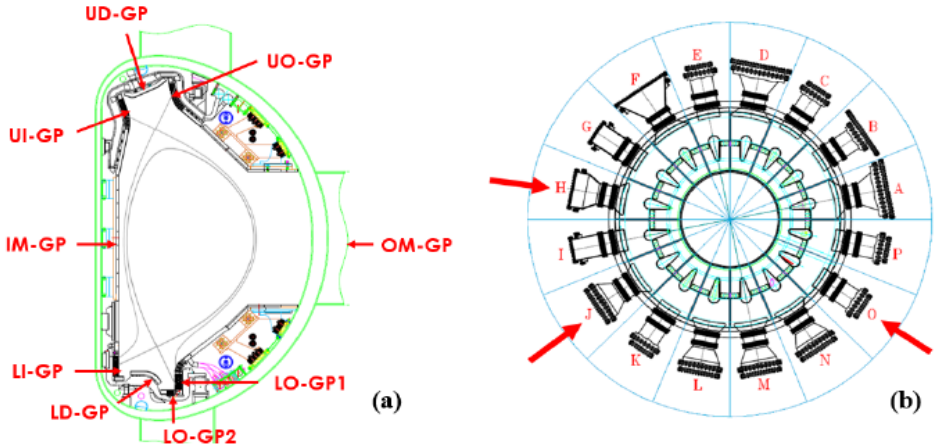

Gas puffing valves distribution in poloidal (left) and toroidal (right) directions on EAST

- Toroidal:
  Port C, O, H
- Poloidal:
  UO,UI,UD,LO,LI,LD,IM

Requests from IAEA-2

- Which **database** services does the community use, need and want?
- Is the interaction of impurity species and/or their derivatives with reactor component surfaces in scope, such as formation and sticking of NHx; vapour formation and interaction with plasma species; etc ?
- How much experimental data is available, in what form, and can it (how can it) be **stored** and curated for future use or analysis?

- EAST ; on going
- LHD ; until FY2022 campaign (it is not clear after FY2023 due to the budget. But Stored data is the data repository